

Ab initio calculations of the self-interstitial in silicon

S. J. Clark and G. J. Ackland

Department of Physics and Astronomy, The University of Edinburgh, Mayfield Road, Edinburgh EH9 3JZ, United Kingdom

(Received 22 November 1996)

Using the *ab initio* pseudopotential approach it is shown that the lowest-energy configuration for the neutral silicon interstitial is the (011) dumbbell. Another local minimum energy atomic configuration with very similar energy was found, which has very low symmetry and hence is multiply degenerate. Other high-symmetry configurations were found to be mechanically unstable. We have further performed *ab initio* molecular-dynamics simulations to study self-interstitial migration. We find several possible mechanisms and a tendency for an atom to become “excited” and perform several correlated jumps through the structure before being recaptured into the minimum energy state. Both excitation and recapture processes appear to be thermally activated, but the number of jumps is larger at low temperatures and the overall migration is athermal. The molecular-dynamics simulations also allow us to evaluate local phonon densities of states for the defects. [S0163-1829(97)04726-7]

I. INTRODUCTION

The structure of the silicon self-interstitial, and its diffusion mechanism, is of great practical and theoretical interest. Nonequilibrium interstitials are often “grown in” during single-crystal growth or generated by irradiation or defect aggregation (notably oxygen), and their migration is strongly linked to the diffusion of other impurities, in particular to boron whose diffusion is strongly enhanced by the presence of self-interstitials. Self-interstitials have also been implicated as the cause of rodlike defects observed in Czochralski single-crystal growth.¹

The study of intrinsic defects in semiconductors has a long history based on empirical force models and more recently on full *ab initio* treatments.² In the case of the silicon self-interstitial, previous results from these two methods are inconclusive. This is not surprising in view of the drawbacks faced by the two methods: The transferability of empirical potentials for silicon is notoriously unreliable, while the scale of calculations required in *ab initio* treatments has meant that full asymmetric relaxation is impossible.

Using empirical force models, Brown and co-workers^{3,4} have advanced the idea of a very delocalized interstitial with a simple migration path through a number of other low-symmetry states. In this paper we report results of an investigation into the possibility of the existence of many such states.

A recent *ab initio* study⁵ examined the tetrahedral and hexagonal interstitial configurations, and another⁶ considered migration down a channel of silicon atoms. Symmetry constraints in that calculation meant that only the prescribed migration route was followed and that other possible mechanisms were neglected. Moreover, symmetry was enforced in relaxing the tetrahedral and hexagonal configurations themselves, and so it is not guaranteed that the high-symmetry configurations were local minima.

A full molecular-dynamics (MD) study of migration⁷ compared the contribution to diffusion from vacancies, interstitials, and concerted exchange, and concluded that the interstitial mechanism was by far the most important.

We have carried out calculations using the *ab initio* density functional theory pseudopotential technique, which allows for full relaxation of the atoms under the Hellmann-Feynman forces. To break any constraints imposed by symmetry, each atom in our starting configuration was slightly displaced from its “ideal” (symmetric) position. The method uses periodic boundary conditions and a plane wave basis which has no bias towards any particular bonding configuration.

We show that the highly symmetric hexagonal and tetrahedral structures are unstable when used as an initial configuration for the defect atom within a perfect diamond lattice and that the stable structures are those in which the interstitial atom forms covalent bonds with other nearby atoms. Thus the channel migration path involves a series of high-energy states and the lowest-energy pathway is likely to be complicated.

II. DETAILS OF CALCULATIONS

We apply density functional theory within the local density approximation^{8,9} for exchange and correlation to periodic supercells of silicon containing defects.^{10,11} A Kleinman-Bylander nonlocal pseudopotential generated by the Kerker¹² method is used to describe the ion-valence electron interactions. The use of periodic boundary conditions allows us to expand the valence electron wave functions in terms of a plane wave basis set. We find that a basis set with a kinetic energy cutoff of 150 eV converges total energy differences to better than 0.001 eV/atom.

We use a 65-atom supercell in the following calculations—this size of supercell allows for atomic relaxation to five shells of atoms surrounding the defect and converges defect formation energies to better than 0.02 eV compared with a single 216-atom calculation. We use a 4-kpt set for Brillouin zone integration which we find converges the total energy to 0.001 eV/atom. We find that the common use of Γ -point sampling in this size of simulation cell does not converge the forces on the atoms to sufficient accuracy to give reliable defect structures. This is not unexpected be-

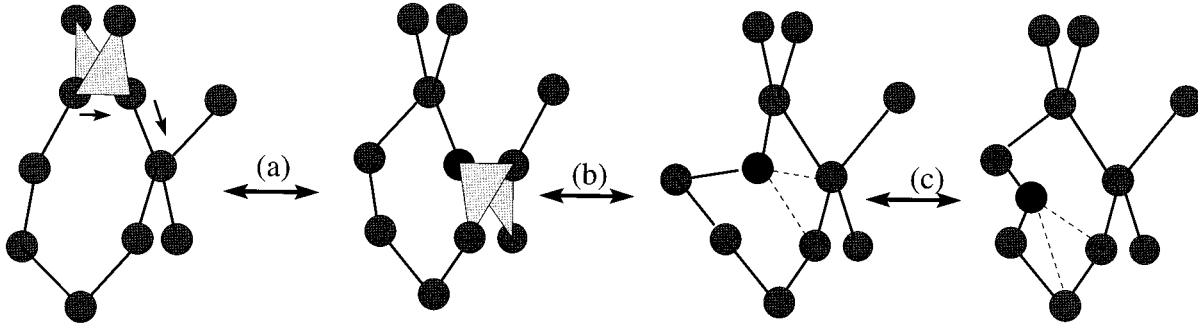


FIG. 1. Schematic pictures of the stable interstitial configurations shown relative to the surrounding atoms of the perfect crystal. In the (110) (left-hand two figures) a pair of atoms replaces a single atom. Each forms a covalent bond to its neighbor along the (110) chain in the direction of the dumbbell. The atoms below the chain remain equidistant from both dumbbell atoms, making them fivefold coordinated and forming a “butterfly” of delocalized charge between the four atoms. The caged interstitial atom (right-hand two figures) attaches covalently between two atoms and relaxes strongly toward the tetrahedral position, thus caged by ten atoms in an asymmetric position. The labeled arrows illustrate the (a) dumbbell-dumbbell, (b) caged-dumbbell, and (c) caged-caged migration processes, all of which are observed in the MD run. The multiply degenerate cage site also allows migration across the cage, directly between second-neighbor sites—the dotted bonds become full covalent bond, while the other bonds to the black atom break. Note that for successive migration via the dumbbell state different atoms are involved in successive steps, whereas for the cage-cage migration the same atom can make several successive jumps.

cause for an eight- or nine-atom unit cell the Γ -point sampling actually gives a negative formation energy.

After placing the defect atom in a given starting configuration we calculate the relaxed electronic structure of the supercell using a preconditioned conjugate gradients algorithm which uses the plane wave expansion coefficients as variational parameters. We calculate the forces on the atoms using the Hellmann-Feynman theorem; the ionic positions are then optimized also by using conjugate gradients to minimize the total energy. This method finds the structure which is the “nearest” local minimum to the starting configuration.

In an attempt to survey more of the phase space of atomic positions, we have also performed finite-temperature *ab initio* molecular dynamics on the system. The classical equations of motion are integrated with a time step of 1.0 fs which we find to be small enough that total energy is conserved without the need for a thermostat. From a relaxed configuration, we give the atoms a random velocity, the total of which corresponds to a kinetic energy equal to twice the required temperature. Within about 100 fs equipartition is observed as the temperature halves with the energy divided between kinetic and potential forms. We allow the system to evolve for a further several picoseconds to observe defect migration.

III. DESCRIPTION OF MINIMUM ENERGY ATOMISTIC CONFIGURATIONS

The lowest-energy configuration which we have found, with a formation energy of 2.16 eV, is a dumbbell interstitial along (011). This is schematically illustrated on the left diagram of Fig. 1. This has been obtained from three different starting configurations by inserting the defect in the otherwise perfect diamond-structure 64-atom supercell: the hexagonal site, the (011) dumbbell, and the (001) dumbbell interstitials (with small initial displacements to break symmetry). The defect is spread over four atoms, as shown in Fig. 1. The five bonds between these four atoms are significantly longer than normal bonds within the crystal; spe-

cifically, the dimer bond along (011) between the two fourfold-coordinated atoms is 2.40 Å, while the four bonds between this dimer and the fivefold-coordinated atoms are 2.46 Å. This compares with an ideal bond length of 2.35 Å. This lengthening is not surprising, since for the neutral defect the five “bonds” contain only eight electrons. In plots of charge density these electrons can be seen to be spread throughout the five bonds.

This configuration is in agreement with the recent approximate molecular orbital calculation¹³ and previous pseudopotential work,⁷ while a similar structure has been found using the empirical Stillinger-Weber potential.³

The second low-energy state which we have found, at 2.29 eV, is rather close in energy to the (011) split state but has a different structure, as shown in the third diagram of Fig. 1. It arose from both the bond-centered and the tetragonal starting configurations. In this case the interstitial is concentrated at a single atom and can be thought of as a distortion from the bond-centered position, with two distinct nearest neighbors (which would be bonded to one another in the absence of the defect). This line of atoms is elastically very unfavorable and becomes strongly buckled, such that the interstitial relaxes toward the tetrahedral site, collecting a shell of five further neighbors as it does so. This configuration is again unstable with respect to a Jahn-Teller distortion which removes all symmetry from the configurations. The interstitial ends up at an asymmetric position within the ten atoms of an adamantane cage, with two normal bonds of 2.32 Å, five longer bonds in the range 2.55–2.82 Å, and three unbonded neighbors at 3.10–3.35 Å. This configuration is henceforth referred to as caged.

This highly asymmetric structure is consistent with empirical calculations with large simulation cells, although the formation energy is significantly lower than that predicted by the Stillinger-Weber model^{14,15} and slightly lower than that predicted with the restricted pair potential model.^{16–18} We presume that this arises because these models do not properly describe large deviations from covalent bonding.

IV. MOLECULAR-DYNAMICS SIMULATIONS: MIGRATION

The two configurations suggest the possibility of diffusion along a (011) chain of atoms. The small energy difference suggests the possibility that such diffusion may be very fast, but that the migration path could be very tortuous. We therefore performed some *ab initio* molecular-dynamics calculations to try to determine the migration path.

Three molecular-dynamics simulations were carried out, at 500, 100, and 1500 K. In each case the simulation cell contained 65 silicon atoms and the volume remained constant. In each case the interstitial was started in the (011) dumbbell position.

Defining a migration jump for an interstitial is rather difficult. Previous authors have followed the rms displacement as a function of time, which is an appropriate measure if there are sufficient jumps to establish a statistical drift. In our simulations, we expect only a few jumps, and so we require a method which will detect a single jump.

We analyzed each step by associating each of the 65 atoms with the nearest of the 64 lattice sites. This means that one site was doubly occupied, and we associated this with the position of the interstitial. A change in the doubly occupied site can then be associated with a migration of the atom.

We tried various other schemes, such as monitoring a map of which atoms are near neighbors (this map turns out to change rapidly and to be extremely complicated, as well as requiring an arbitrary definition of near neighbor) and relaxing the MD configuration at each time step using an empirical potential (empirical potentials tend to have different energy minima), but the site-association analysis, described above, was the most useful analysis tool.

At 500 K the doubly occupied site remained in its initial location for the entire run of 5 ps.

At 1000 K we found a single event at which one of the dumbbell interstitial pairs moved to an adjacent site, followed by a series of five correlated jumps of the same atom to other sites, and final recapture. All these jumps occurred in a period of 0.175 ps in the middle of a 5-ps simulation. The only other ‘‘jumps’’ suggested by our method were an oscillation back and forth between adjacent two sites which appears to be an excitation from the dumbbell into the caged site [migration (b) in Fig. 1] which is equidistant between two lattice sites. There was one such event in the 1000-K simulation and four in the 1500-K simulation.

At 1500 K a number of jumps were observed, including several caged-site excitations, as described above, and a few single migration events followed by a lengthy residence of the interstitial in the new site.

To determine the nature of the jumps, MD positions at the time step indicated as a migration event were used as starting configurations for static minimization. One rather surprising result of this was the relaxation to a hexagonal interstitial with energy 2.45 eV. This configuration was not metastable when the interstitial atom was inserted into the hexagonal site of the perfect crystal—we find that it is actually stabilized by the relaxation of the six adjacent atoms and therefore could not be found from initial static calculations without enforced symmetry.

Closer examination of the migration suggested that no

single pathway was favored. Indeed the interstitial did not always jump between nearest-neighbor sites, preferring on several occasions to move across the adamantane cage to next-nearest-neighbor sites via the hexagonal site. In Fig. 1 we show the three main migration paths. In (a) migration occurs directly between dumbbell configurations and the atoms involved in the interstitial change. In (b) migration goes from dumbbell to cage with one of the dumbbell atoms becoming identified as the interstitial. In (c) the atom moves across the cage to another position. This is the type of jump which need not be between nearest neighbors. Unlike path (a), the same atom is the interstitial before and after the migration.

Based on the frequency that each migration route occurs in out MD simulations, the lowest barrier, by far, appears to be for jumps of type (c). However, because these do not involve the lowest-energy configuration, this kind of jump can only occur after a jump of type (b). The correlated jumps appear to be started with a type (b), followed by a series of type (c), and a final (reversed) type (b). Direct migration between dumbbell configurations of type (a) are the rarest but are important because they cause the identity of the interstitial to change.

V. MOLECULAR-DYNAMICS SIMULATIONS: FREE ENERGY

To investigate the effect of the interstitial on the vibrational spectrum we evaluated the density of occupied phonon

Densities of States from 500K run

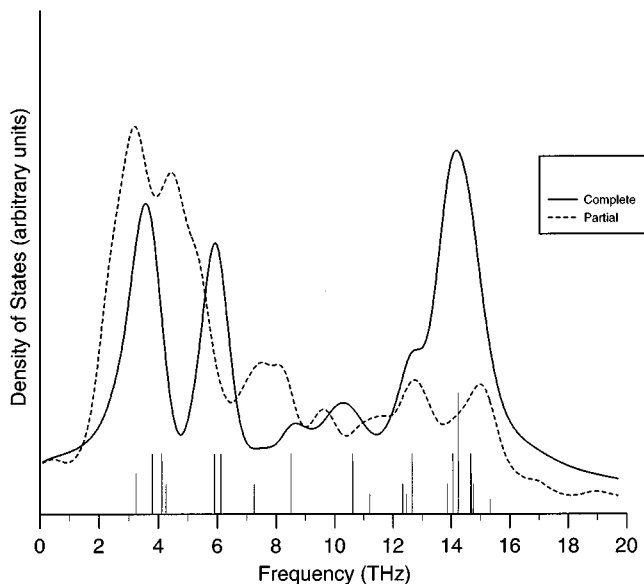


FIG. 2. The average local occupied phonon density of states, $g_i(\omega)$, projected onto the 63 nondumbbell atoms and the two atoms comprising the dumbbell, from the molecular-dynamics run at 500 K. Tick marks show zone-center normal-mode frequencies calculated for a 64-atom cubic unit cell at 0 K using standard *ab initio* lattice dynamics, with amplitudes proportional to the degeneracy of each mode.

states projected onto each atom from the Fourier transform of the velocity autocorrelation function:

$$g_i(\omega) = 3 \frac{\int_t v_i(0)v_i(t)e^{i\omega t} dt}{\int_w \int_t v_i(0)v_i(t)e^{i\omega t} dt},$$

where $v_i(t)$ is the instantaneous velocity of the i th particle at time t , from which we define a local free energy at each atom:

$$F_i = -kT \ln \left(\int g_i(\omega) d\omega \right).$$

From examining these, we find that the local free energy is smaller for the dumbbell atoms.

For the short simulation times here, we do not expect these densities of states to be very accurate. However, in each case it is clear that the densities of states projected onto the interstitial atoms are missing the high-frequency peak which corresponds to bond stretching. The graphs from the 500 K run, which are not complicated by migration events, are shown in Fig. 2. This is in contrast to previous work^{15,16} which has suggested that the interstitial should be associated with high-frequency vibrational modes. The absence of these modes is the main reason for the vibrational entropy associated with the interstitial.⁷

We have also calculated the equivalent set of frequencies for a perfect 64-atom cell by static displacements.¹⁹ Only 192 normal modes exist for this cell, the frequencies and degeneracies of which are shown in Fig. 2. The density of occupied phonon states is expected to consist of these modes, plus any associated with the interstitial, broadened by temperature. Comparing free energies per atom from the static calculation with the dynamic one suggests a small vibrational entropic contribution to free energy for the (011) dumbbell.

VI. CONCLUSIONS

Static relaxation using a fully *ab initio* approach has shown that the lowest-energy configuration for the silicon

interstitial is the (110) split dumbbell, although a highly asymmetric configuration with a single atom on one side of an adamantane cage is close in energy.

Molecular-dynamics simulations show that there is no simple single migration path, but that migration tends to occur by excitation of a single atom, which can then travel significant distances through the open diamond structure prior to recapture. The distance traveled by the interstitial was observed to be greater at lower temperature, but the number of excitations was greater at high temperature.

Insufficient events were observed to give reliable data for migration energies. However, we were able to define the mechanism which appears to be one of thermally activated excitation to a fast migrating state, followed by thermally activated recapture of the single migrating atom. The net effect of these two processes is frequent, short migration at high temperatures and infrequent, long migration at low temperatures. This is consistent with the experimental observation that migration energy is approximately athermal.

Consideration of the vibrational spectrum showed that the bond-stretching modes are absent when projected onto the interstitial atoms. Thus the vibrational free energy of the interstitial is lower than for a bulk atom; this is in contrast to the situation found with most empirical potential studies and will tend to favor interstitial formation.

ACKNOWLEDGMENTS

S.J.C. would like to thank EPSRC for financial support and G.J.A. thanks BP and the Royal Society of Edinburgh for financial support. We have also received assistance from the Edinburgh Parallel Computing Centre on whose Cray-T3D the calculations were performed. The authors thank S. Breuer of the EPCC for useful discussions. These calculations were carried out using the CETEP code in collaboration with UKCP consortium, details of which can be found at <http://gserv1.dl.ac.uk/TCSC/projects/UKCP/ukcp.html>.

¹S. Takeda, M. Kohyama, and K. Ibe, *Philos. Mag. A* **70**, 287 (1994).

²D. Maroudas and S. T. Pantelides, *Chem. Eng. Sci.* **49**, 3001 (1994).

³T. Sinno, Z. K. Jiang, and R. A. Brown, *Appl. Phys. Lett.* **68**, 3028 (1996).

⁴D. Maroudas and R. A. Brown, *Appl. Phys. Lett.* **62**, 172 (1993).

⁵D. J. Chadi, *Phys. Rev. B* **46**, 9400 (1992).

⁶P. J. Kelly and R. Car, *Phys. Rev. B* **45**, 6543 (1992).

⁷P. E. Blochl, E. Smargiassi, R. Car, D. B. Laks, W. Andreoni, and S. T. Pantelides, *Phys. Rev. Lett.* **70**, 2435 (1993).

⁸J. P. Perdew and A. Zunger, *Phys. Rev. B* **23**, 5048 (1981).

⁹D. M. Ceperley and B. J. Alder, *Phys. Rev. Lett.* **45**, 566 (1980).

¹⁰L. J. Clarke, I. Stich, and M. C. Payne, *Comput. Phys. Commun.*

72, 14 (1992).

¹¹M. C. Payne, M. P. Teter, D. C. Allan, T. A. Arias, and J. D. Joannopoulos, *Rev. Mod. Phys.* **64**, 1045 (1992).

¹²G. P. Kerker, *J. Phys. C* **13**, L189 (1980).

¹³A. Mainwood, *Mater. Sci. Forum* **196**, 1589 (1995).

¹⁴M. Nastar, V. Bulatov, and S. Yip, *Phys. Rev. B* **53**, 13 521 (1996).

¹⁵F. H. Stillinger and T. A. Weber, *Phys. Rev. B* **31**, 5262 (1985).

¹⁶S. J. Clark and G. J. Ackland, *Phys. Rev. B* **48**, 10 899 (1993).

¹⁷G. J. Ackland, *Phys. Rev. B* **44**, 3900 (1991).

¹⁸G. J. Ackland, *Phys. Rev. B* **40**, 10 351 (1989).

¹⁹H. C. Hsueh, M. C. Warren, H. Vass, G. J. Ackland, S. J. Clark, and J. Crain, *Phys. Rev. B* **53**, 14 806 (1996).